PROCEEDINGS OF SCIENCE

High-p_T results from STAR - what did we learn?

Jana Bielcikova for the STAR Collaboration*
NPI ASCR, Rez, 160 68, Czech Republic
E-mail: jana.bielcikova@ujf.cas.cz

We report recent results on medium modification of two and three-particle correlations in heavy-ion collisions at RHIC measured by the STAR experiment. In particular, properties of an additional extended correlation in pseudo-rapidity, the ridge, not present in p+p or d+Au collisions, are discussed. Further shape modification of the away-side correlation peak at intermediate-p_T is investigated to look for possible signals of conical emission. Finally, the system size dependence of two-particle correlations with large transverse momentum is presented and compared to energy loss model predictions.

High-pT Physics at LHC -09
February 4- 7 2009
Prague, Czech Republic

*Speaker.

PoS(High-pT physics09)016

One of the main goals of experimental program at the Relativistic Heavy Ion Collider (RHIC) at Brookhaven National Laboratory is investigation of nuclear matter under extreme conditions of high temperature and energy density created in laboratory collisions of two heavy ions at high energies. The particle production in central Au+Au collisions at top RHIC energy ($\sqrt{s_{NN}}$ =200 GeV) is suppressed by about a factor of five with respect to p+p collisions scaled by the number of binary nucleon-nucleon collisions [1, 2, 3, 4]. This suppression, usually referred to as *jet quenching*, is present both in inclusive particle spectra as well as in di-hadron correlations at high transverse momentum (p_T) [5]. These observations indicate energy loss and/or modified fragmentation of high momentum partons in the system produced in central Au+Au collisions.

Compared to the measurements of inclusive particle production, studies of jets and their modification are expected to provide higher sensitivity to the medium properties. Since a direct measurement of jets in heavy-ion collisions at RHIC is difficult due to the large number of produced background particles and the first measurements of directly reconstructed jets have emerged only recently [6, 7], azimuthal correlations of particles with large p_T have been commonly used to study the jet related processes instead. Studies of di-hadron azimuthal correlations in central Au+Au collisions revealed several noticeable differences to measurements in p+p and d+Au collisions. The near-side correlation in heavy-ion collisions differs from that measured in p+p or d+Au collisions. The near-side 'jet-like' component is localized at small azimuthal ($\Delta\phi$) and pseudo-rapidity ($\Delta\eta$) angular differences as in elementary collisions, but in addition a new correlation extended in pseudo-rapidity, the *ridge*, has been observed in central Au+Au collisions [8]. Also the away-side correlation peak in Au+Au collisions differs from that measured in p+p or d+A collisions. The observed disappearance of the away-side correlation peak for charged trigger particles with $p_T^{trig} >$ 4-6 GeV/c and associated charged particles with $p_T^{assoc} >$ 2 GeV/c in central Au+Au collisions [9] is accompanied by an enhanced production of associated particles with lower transverse momenta $p_T^{assoc} >$ 0.15 GeV/c and a strong ('double-hump') shape modification of the away-side peak [10]. At high transverse momenta $p_T^{assoc} >$ 4 GeV/c, both near and away side correlation peaks resemble again those in elementary collisions, but the yield of away-side associated particles is suppressed to the level of inclusive particle production [5].

In this paper we report recent progress on measurements of azimuthal ($\Delta\phi$) and pseudo-rapidity ($\Delta\eta$) correlations from the STAR experiment at RHIC ($\sqrt{s_{NN}}$ = 200 GeV) using two and three-particle correlation techniques, identified particles and different collision systems (d+Au, Cu+Cu, Au+Au) in order to obtain more insight into the particle production mechanism and energy loss at RHIC.

1. Near-side correlation: the ridge

To quantify the strength of the ridge-like correlations, the measured near-side di-hadron correlation is decomposed into a jet-like component centered at $(\Delta\phi, \Delta\eta) \sim (0,0)$ and a ridge component extended in $\Delta\eta$ on top of an elliptic flow (v_2) modulated background. For analysis details see e.g. Ref. [8].

The centrality, system size and collision energy dependences of the ridge yield were measured in STAR for several trigger particle species and are discussed in detail in [11, 12] and elsewhere in these proceedings [13]. Here, we only mention that for all studied trigger particle species the

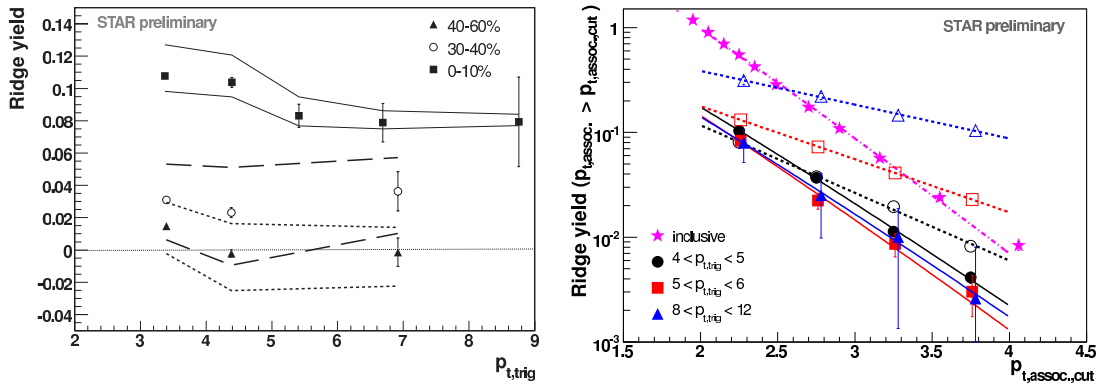

Figure 1: The transverse momentum dependence of the ridge yield in Au+Au collisions at $\sqrt{s_{NN}}$ = 200 GeV in $|\Delta\eta| < 1.7$. (Left) Ridge yield as a function of p_T^{trig} for 2 GeV/c < p_T^{assoc} < p_T^{trig} and three centrality bins. The lines are systematic uncertainties due to the elliptic flow subtraction. (Right) Transverse momentum spectra of charged particles associated with ridge (solid symbols) compared to those in the jet-like component (open symbols) and inclusive particle p_T spectrum (stars). The ridge and jet spectra are shown for several p_T^{trig} ranges in central (0-12%) Au+Au collisions. The inclusive charged particle spectrum corresponds to 0-5% central Au+Au collisions. The lines are exponential fits to the measured p_T^{assoc} spectra [8].

yield of charged particles associated with the ridge shows a significant increase by about a factor of four going from d+Au to central Au+Au collisions. At a given N_{part} and collision energy the ridge is however independent of the collision system within errors. In contrast, the jet-like yield at given $\sqrt{s_{NN}}$ is, within errors, independent of centrality and collision system and is consistent with that measured in d+Au collisions. Both the ridge and jet-like yields are considerably smaller in collisions at $\sqrt{s_{NN}}$ = 62 GeV than at $\sqrt{s_{NN}}$ = 200 GeV, but the ratio of the two yields remains independent of collision energy. In this paper we focus on further detailed properties of the ridge in Au+Au collisions at $\sqrt{s_{NN}}$ = 200 GeV, where the ridge amplitude is largest and where the largest data volume is available.

The left panel of Figure 1 shows the dependence of the ridge yield on the transverse momentum of trigger particles, p_T^{trig}, for charged di-hadron correlations in three centrality bins in Au+Au collisions at $\sqrt{s_{NN}}$ = 200 GeV [8]. The associated charged particles were selected with transverse momentum 2 GeV/c < p_T^{assoc} < p_T^{trig}. In peripheral collisions the ridge yield is negligible but increases with centrality. In central collisions the ridge yield is approximately independent of p_T^{trig} and persists up to $p_T^{trig} \approx 8$ GeV/c limited by the statistics of available data. The fact that the ridge exists in the p_T domain where parton fragmentation governs the particle production could indicate that its physical origin is associated with jet production. The high statistics data collected in Run 7 at RHIC will extend the reach in p_T^{trig} and thus bring further knowledge at even higher p_T^{trig}.

A detailed study of the p_T spectra of particles associated with the ridge in different p_T^{trig} windows is presented in the right panel of Figure 1 [8]. The spectra are compared to the p_T spectra of particles produced in the bulk and also to those associated with the near-side jet-like component. The inverse slope extracted from an exponential fit to the p_T spectra for the ridge-like yield is independent of p_T^{trig} and only sligthly larger (by $\approx$ 50 MeV) than that of the inclusive charged particle p_T spectrum. Contrary to this observation the jet-like yield has a significantly harder spectrum with

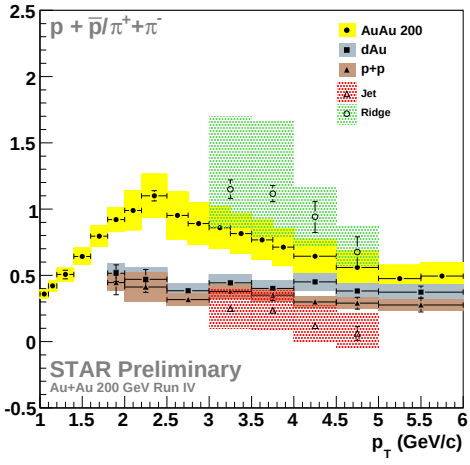

Figure 2: Proton/pion ratios in the ridge (open circles) and jet-like component (open triangles) compared to the inclusive particle ratios in p+p (solid triangles), d+Au (solid square) and Au+Au (solid circles) collisions measured at $\sqrt{s_{NN}}$ = 200 GeV [14].

an inverse slope increasing steeply with p_T^{trig}, in line with jet fragmentation.

Next we discuss the particle composition of the ridge. The baryon/meson ratios in both non-strange and strange quark sectors measured at RHIC, steeply increase with p_T up to about $p_T \approx 3$ GeV/c, where the enhancement of baryon/meson production reaches its maximum value of about three relative to p+p collisions [4]. A decrease of the baryon/meson ratio is observed for $p_T > 3$ GeV/c and the baryon/meson ratio eventually reaches the value measured in p+p collisions at $p_T \approx 6$ GeV/c. This finding can be rather successfully explained in the framework of parton recombination and coalescence. A study of baryon/meson ratios in the ridge could therefore help to quantify what role the recombination and coalescence production mechanisms play in its origin. The measured data of p/π as well as Λ/K^0_S ratios [11, 12, 14] show that the baryon/meson ratios in the ridge are enhanced with respect to those in the elementary collisions. This is demonstrated in Figure 2 where the p_T dependence of p/π ratio in the ridge is shown together with the values in the jet-like component and inclusive p_T spectra in Au+Au and p+p collisions [14]. The baryon/meson ratio in the ridge is similar to that from the inclusive measurements in Au+Au collisions contrary to the jet-like component where the p/π ratios agrees with that measured in p+p and d+Au collisions. This observation thus supports ridge models where hadronization is based on parton recombination [15, 16].

Additional information on the physical origin of the ridge can be obtained from the analysis of di-hadron correlations with respect to the orientation of event plane. In particular, selecting the trigger particle with a given azimuthal angular difference with respect to the event plane (ϕ_s), path length effects on di-hadron correlations and their individual components can be investigated. Figure 3 shows the measurement of the event plane dependence of the ridge and jet-like yields in Au+Au collisions at $\sqrt{s_{NN}}$ = 200 GeV [17]. While the jet-like yield is approximately constant or only slightly increases with ϕ_S, the ridge yield reveals what may be interpreted as path length effects. In the event plane, the ridge yields for both semi-central (20-60%) and central (0-5%) Au+Au collisions are similar in magnitude, but in semi-central collisions the ridge yield is found to decrease more steeply with ϕ_s. This observation could imply a strong near-side "jet"-medium interaction in the event plane resulting in the ridge formation and a minimal interaction perpendicular to the event plane in semi-central collisions. In central collisions, the ridge remains large in

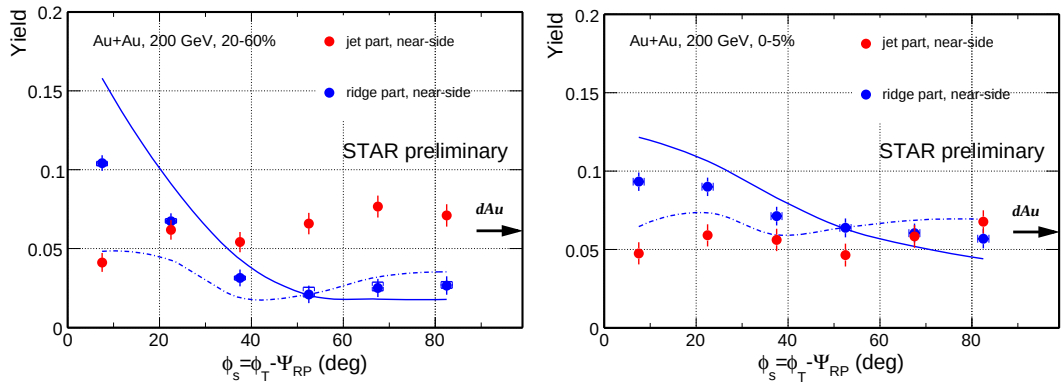

Figure 3: Ridge and jet-like yields from near-side di-hadron correlations in 20-60% (left) and 0-5% (right) Au+Au collisions at $\sqrt{s_{NN}}$ = 200 GeV as a function of the angular difference ϕ_s between the trigger particle and the event plane. The results are for $3 < p_T^{trig} < 4$ GeV/c and $1.5 < p_T^{assoc} < 2$ GeV/c. The yields are extracted in $|\Delta\eta| < 0.7$ and $|\Delta\phi| < 1$. The lines indicate systematic uncertainties due to the elliptic flow subtraction procedure [17].

the direction perpendicular to the orientation of the event plane, but its ϕ_s dependence is much less pronounced which reflects an almost symmetric shape of the collision zone.

We close the discussion on measured ridge properties with studies using three-particle correlations ('1+2 correlations') in pseudo-rapidity in order to examine possible fine structure of the ridge. By selecting one trigger particle and two associated particles, two pseudo-rapidity angular differences $\Delta\eta_{1(2)} = \eta^{trig} - \eta^{assoc1(2)}$ are calculated. Trigger particles (charged particles with p_T^{trig} = 3-10 GeV/c) and associated charged particles with p_T^{assoc} =1-3 GeV/c were used to look for substructures in $(\Delta\eta_1, \Delta\eta_2)$ distributions, which are displayed in Figure 4. For further details on the analysis method, background subtraction technique, and systematic error evaluation we refer the reader to [18]. A clear jet-like peak is present at $(\Delta\eta_1, \Delta\eta_2) \sim (0,0)$ in both d+Au and Au+Au collisions. In addition, a uniform overall excess of pairs of associated charged particles is observed

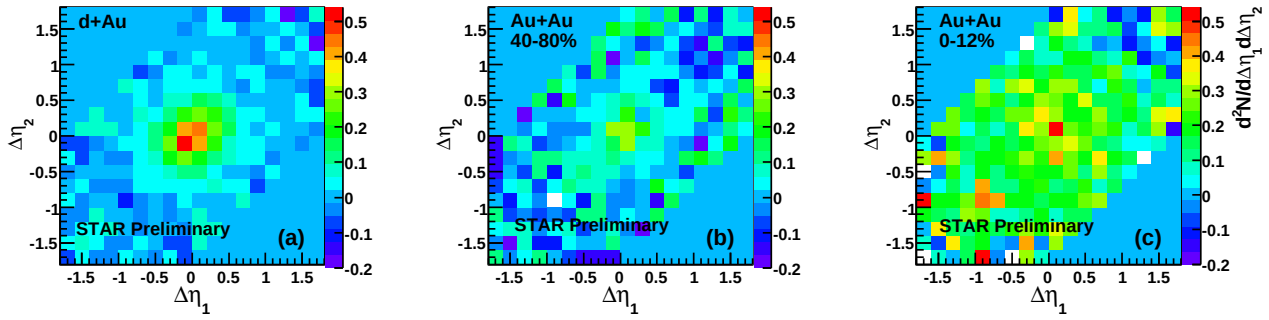

Figure 4: Three-particle correlations in $\Delta\eta$ for small azimuthal angle difference ($\Delta\phi < 0.7$) between associated particles and trigger particle measured by STAR for (a) minimum bias d+Au collisions, (b) 40-80% Au+Au collisions and (c) 0-12% central Au+Au collisions at $\sqrt{s_{NN}}$ = 200 GeV [18].

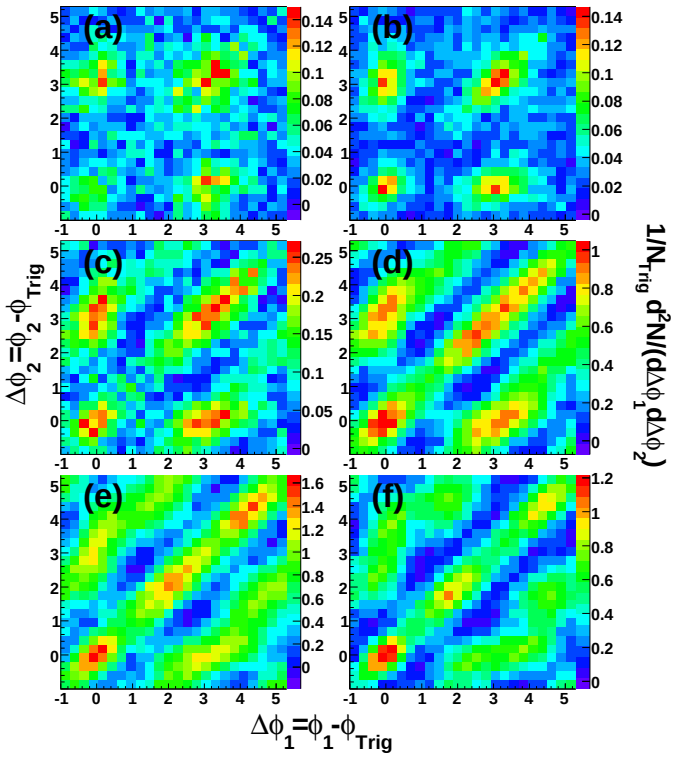

Figure 5: Three-particle azimuthal correlations obtained after background subtraction using the 'jet-flow background subtraction method' in (a) p+p, (b) d+Au, (c) 50-80%, (d) 30-50%, (e) 10-30%, and (f) 0-12% Au+Au collisions at $\sqrt{s_{NN}}$ = 200 GeV [39].

in central Au+Au collisions. A closer look at on-diagonal, off-diagonal, radial and angular projections confirmed this observation and showed that within errors no significant correlation exists between the particles in the ridge (cf. [18]). The absence of horizontal and/or vertical strips in the three-particle correlations could indicate that the coexistence of the ridge and the jet fragmentation in vacuum is small. Further studies with higher statistics are needed to confirm this observation.

The observation of the ridge has triggered a lot of interest in the theoretical community leading to numerous models which attempt to explain the physical origin of the ridge. These models include parton recombination in the medium [19, 15], strong longitudinal flow expansion causing in-medium broadening of gluon radiation [20], spontaneous formation of extended color fields in longitudinally expanding medium [21], momentum kicks to partons along the jet propagation direction in the medium [22], jet quenching combined with strong radial flow [23, 24, 25], glasma flux tubes [26, 27] and several other mechanisms. More quantitative model predictions as well as further studies of the particle composition of the ridge, studies at forward rapidities, investigation of three-particle $(\Delta\eta_1, \Delta\eta_2)$ correlations, and searches for the ridge in direct γ triggered correlations will bring further insight into the physical origin of the ridge.

2. The away-side peak: shape modification and path length effects

Detailed studies of the away-side peak in di-hadron correlations in Au+Au collisions at $\sqrt{s_{NN}}$=200 GeV found that its shape is strongly modified by the presence of the medium created in central heavy-ion collisions at RHIC. The shape of the away-side peak strongly depends on both p_T^{trig} and p_T^{assoc} of charged particles involved in the correlation studies. In central Au+Au collisions, it has

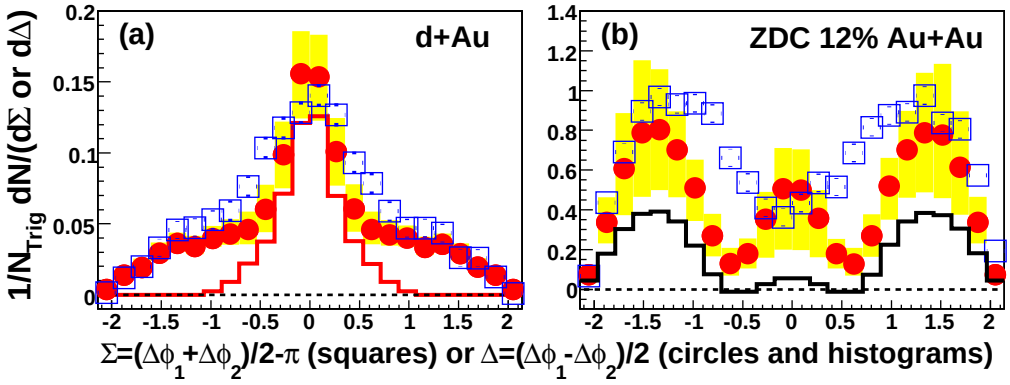

Figure 6: Projections of away-side three-particle correlations along the diagonal (squares) and off-diagonal (circles) in (a) d+Au and (b) 0-12% central Au+Au collisions at $\sqrt{s_{NN}}$ = 200 GeV [39]. The shaded (yellow) areas correspond to systematic uncertainities in the off-diagonal projections. The solid curve in (b) shows the 3-particle cumulant result in azimuthal angle relative to reaction plane.

been observed that in the intermediate p_T range the away-side peak has a double-hump structure with a minimum around $\Delta\phi \approx \pi$ [10, 28] instead of a Gaussian shaped as commonly observed in p+p or d+Au collisions. This observation triggered a lot of interest, both experimental and theoretical. Already in the 1970's it was postulated that a Mach cone or wake field could be created by a propagating high-p_T parton in a dense medium [29, 30] which would be reflected in di-hadron correlations as a double-hump structure in the away-side peak. However, the observed shape modification might also be a consequence of large angle gluon radiation, deflection of jets by radial flow, or Čerenkov gluon radiation [31, 32, 33, 34].

In order to discriminate among various production mechanisms it is therefore necessary to study azimuthal three-particle correlations. Similar to the case of three-particle correlations in pseudo-rapidity presented in Section 1, one trigger and two associated particles are selected but now the correlation function is expressed in terms of two relative azimuthal angles $\Delta\phi_1$ and $\Delta\phi_2$, between the trigger particle and each of the associated particles. Conical emission would lead to two peaks, one at $\Delta\phi_1 = \pi \pm \theta$ and the other one at $\Delta\phi_2 = \pi \pm \theta$, with the cone angle θ which is connected to the sound velocity in the produced medium. Below we present results based on two different methods: jet-flow background subtraction method and three-particle cumulant method.

The first method is a two component method based on a measurement of three-particle density normalized per trigger particle [35, 36, 37, 38, 39]. It includes explicit subtraction of v_2 and v_4 contributions using the Zero Yield At 1 radian (ZYA1) method [40, 39]. The resulting correlations in p+p, d+Au and Au+Au collisions at $\sqrt{s_{NN}}$=200 GeV are shown in Figure 5 [39]. Notice first that the away-side peak is elongated along the diagonal and this elongation increases from p+p to central Au+Au collisions. This implies that the away-side particle pairs stay relatively close to each other while their angles vary over a rather broad range. In central Au+Au collisions additional off diagonal structures around ($\pi \pm 1.37$, $\pi \mp 1.37$) are also present. A closer look at on- and off-diagonal projections is presented in Figure 6 for d+Au and central Au+Au collisions [39]. In central Au+Au collisions the off-diagonal peaks are prominent and their origin could be linked to conical emission. The side peaks in the diagonal projection contain other contributions besides

the conical emission contributions which could originate from k_T broadening, large angle gluon radiation, and/or deflected jets. To quantify the angular distance θ of the off-diagonal peaks from π, the projections were fitted with three Gaussian peaks. It was found that the value of θ is on average $1.37 \pm 0.02(\text{stat})^{+0.06}_{-0.07}(\text{syst})$ and is within errors independent of centrality and p_T^{assoc}. If the observed conical emission pattern is due to Mach-cone shock waves, then the extracted value of θ reflects the speed of sound in the medium over the entire evolution of the collision. In [41] it was suggested that statistical global momentum conservation influences the shape of the three-particle correlation functions. However, the predicted three-particle correlation from statistical global momentum conservation [41] is inconsistent with data [39].

The second method used in STAR is based on three-particle cumulants and unlike the first method, it is a fully model independent method based on measured three-particle densities from which combinatorial terms are subtracted based on measured two- and one-particle densities [42, 43, 44]. Figure 7 shows the centrality dependence of the three-particle cumulant in Au+Au collisions. The data show four prominent peaks at (0,0), (π,π), (0,π), and (π,0). In addition there are weaker peaks positioned at regular intervals which are strongest in semi-central collisions (10-30%), where v_2 and v_4 flow Fourier coefficients are also the largest. This could be qualitatively understood as arising from irreducible non-diagonal collective flow contributions of the order $v_2v_2v_4$ [42]. Parameterizing the measured v_2 and v_4 values yields amplitudes compatible with those observed in the data. While the presence of the near- and away-side peaks can be a result of jet emission alone, they may also result from the interplay of jet correlations with the event plane and collective flow. As for the previous method, we examine in detail the projections of the

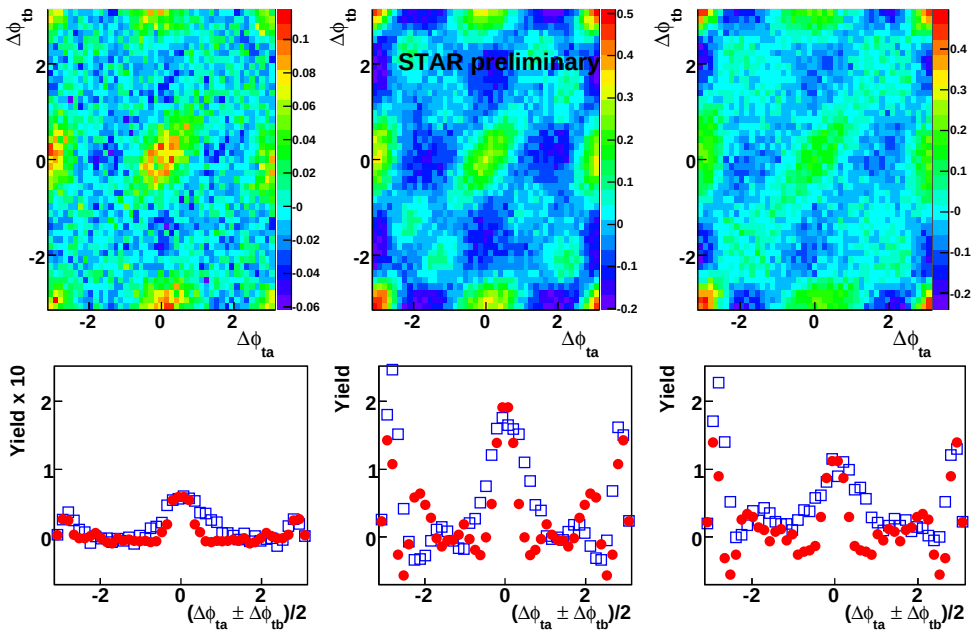

Figure 7: 3-particle cumulants (top row) for 50-80% (scaled x 10) (left), 10-30% (middle) and 0-10% (right) Au+Au collisions together with projections (bottom row) along the main (blue squares) and alternate diagonals (red circles) [43].

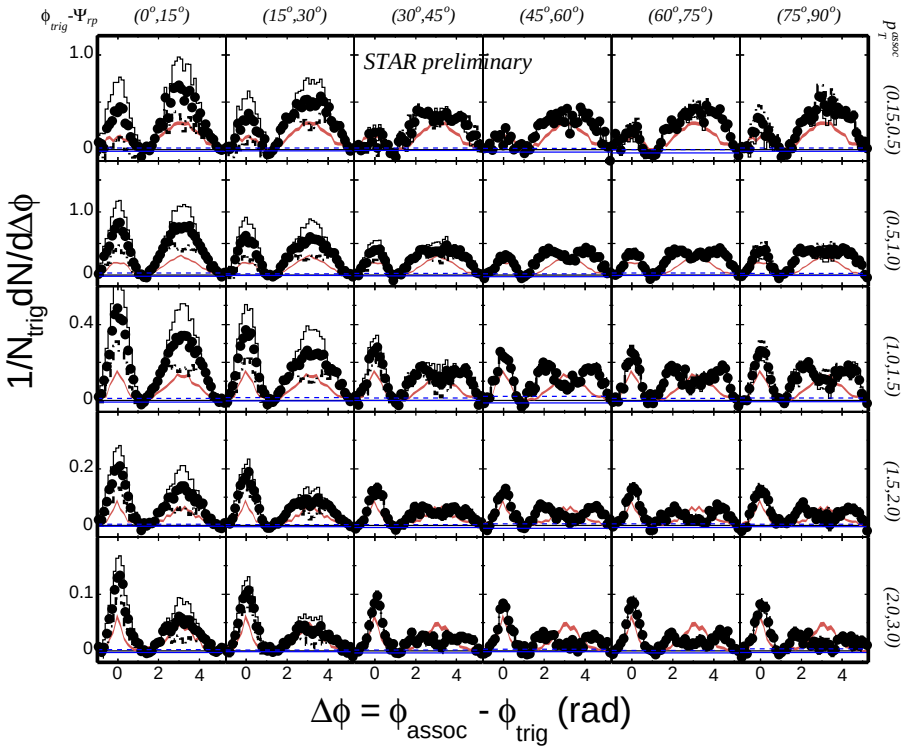

Figure 8: Di-hadron correlations as a function of $\phi_s = \phi_{trig} - \Psi_{EP}$ and p_T^{assoc} for $3 < p_T^{trig} < 4$ GeV/c in 20-60% Au+Au collisions at $\sqrt{s_{NN}}$ [17]. The ϕ_s range increases from 0-15° (left column) to 75-90° (right column); the p_T^{assoc} range increases from 0.15-0.5 GeV/c (top row) to 2-3 GeV/c (bottom row). The histograms and dashed lines indicate the systematic uncertainties from elliptic flow and background normalization, respectively. The red lines are the corresponding di-hadron correlation function in d+Au collisions.

three-particle cumulants which are displayed at the bottom of Figure 7. Although the projections demonstrate structures consistent with $v_2v_2v_4$ terms and no clear evidence for conical emission is observed the possibility that conical emission is masked by flow terms, or is too weak to be visible in this analysis, is not excluded. We note that the cumulants from this analysis use azimuthal angle measured in the laboratory frame. Three-particle cumulant analyzed in azimuthal angle relative to event plane, shown in the histogram in Figure 6(b), indicates conical emission.

Path length effects on the away-side correlation are similarly investigated as was done for the near-side correlation. Figure 8 displays the background subtracted di-hadron correlations as a function of ϕ_s and p_T^{assoc} [17]. The shape of the away-side correlation evolves from a single Gaussian peak to a double peak as ϕ_s increases from in-plane ($\phi_s \sim 0°$) to out-of-plane ($\phi_s \sim 90°$) for most p_T^{assoc} bins studied. To quantify the modification of the away-side peak, in Figure 9 the RMS of the away-side correlation function for $|\Delta\phi - \pi| < \pi - 1$ for central (0-5%) and semi-central (20-60%) Au+Au collisions is shown [17]. The away-side distribution broadens with increasing ϕ_s, but this broadening is weaker in central Au+Au collisions. For $\phi_s \sim 0°$ the RMS in semi-central Au+Au collisions is comparable to that in d+Au collisions, while in central Au+Au collisions it displays a noticeable broadening relative to d+Au collisions. This could be qualitatively understood

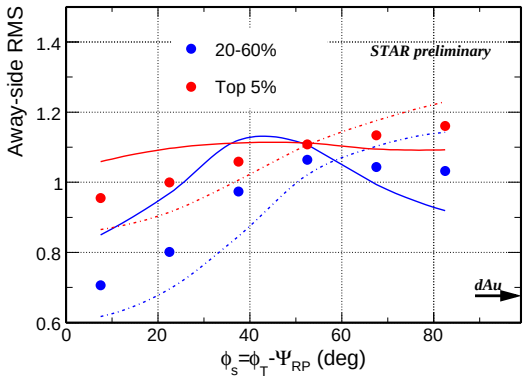

Figure 9: The RMS of the away-side correlation functions as a function of the angle of the trigger particle relative to the orientation of the event plane (ϕ_s) in 20-60% (blue) and top 5% (red) Au+Au collisions at $\sqrt{s_{NN}}$ = 200 GeV [17]. The trigger p_T range is $3 < p_T^{trig} < 4$ GeV/c and the associated particle p_T range is $1 < p_T^{assoc} < 1.5$ GeV/c. The curves indicate systematic uncertainties due to elliptic flow subtraction. The corresponding d+Au result is indicated by the arrow.

as a consequence of different path lengths that the away-side parton traverses in-plane for the two studied centralities. On the other hand, the RMS values out-of-plane are not much different between the two centralities, which is again consistent with the collision geometry as the path lengths perpendicular to the event plane are similar.

3. System size dependence of di-hadron correlations with large p_T

The ultimate goal of the heavy-ion experimental program at RHIC is to determine the properties of the hot and dense medium created in heavy-ion collisions. Several theoretical calculations of partonic energy loss in the nuclear medium have been used to derive quantities characterizing the medium properties such as the transport coefficient $\hat{q}$ corresponding to the average momentum kick per mean free path of the parton. In general, the energy loss of individual partons is different for light quarks (u, d, s), heavy quarks (c, b) and gluons due to the QCD color factor and the dead cone effect. In addition, the energy loss depends on the path length L the parton traverses through the medium. For radiative energy loss, which is thought to be dominant for light quarks, the energy loss depends on L^2 due to coherence effects [45, 46, 47]. On the other hand, for elastic scattering energy loss a linear dependence on L is expected [48]. Finally, a realistic calculation must also incorporate fragmentation, collision geometry and time evolution of the medium. The combination of measurements of suppression observed in inclusive particle p_T spectra with di-hadron suppression on the away side is expected to provide better sensitivity to the model parameters [49, 50]. Below, we present results of the system size dependence of di-hadron correlations at high-p_T in Cu+Cu and Au+Au collisions at $\sqrt{s_{NN}}$ =200 GeV and compare them to those measured in d+Au collisions where no hot and dense medium is formed.

The system size dependence of the near-side associated-particle yield in $|\Delta\eta| <$0.7 and $|\Delta\phi| <$ 0.7 is presented as a function of number of participants (N_{part}) in Figure 10 [51]. It is observed that the near-side associated yields in Cu+Cu and Au+Au collisions are consistent within errors for

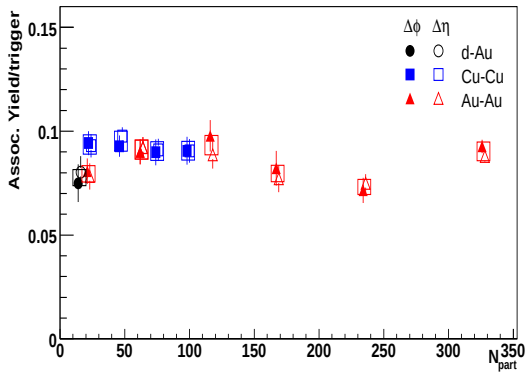

Figure 10: Centrality dependence of the near-side yield of charged particles associated (3 GeV/$c < p_T^{assoc} <$ p_T^{trig}) with charged trigger particles of 6 GeV/$c < p_T^{trig} <$ 10 GeV/c [51]. The open symbols are horizontally offset for clarity.

similar N_{part} and within errors agree with those measured in d+Au collisions. The independence of the near-side associated yields on centrality indicates that in the studied p_T range fragmentation is largely unmodified by the presence of the medium and partons likely fragment outside the medium after energy loss.

Although di-hadron correlations are more sensitive to the central part of the medium, the choice of a high-p_T trigger particle still leads to a surface bias in the distribution of hard scattering points [49]. Consequently, the away-side parton has a longer path length through the medium and the measurements of the away-side associated yields provide an important tool for studying the path length dependence of energy loss. After subtracting the elliptic flow contribution the away-side associated yield is calculated in the azimuthal range $|\Delta\phi - \pi| < 1.3$ covering the range of the away-side jet. The nuclear modification factor I_{AA}, which has been calculated in our case as the ratio of the away-side associated yield in A+A collisions with respect to d+Au collisions, is shown in Figure 11 [51]. For both Cu+Cu and Au+Au collision systems the away-side yield is suppressed relative to d+Au collisions and the amount of the suppression increases with N_{part}. Despite the differences in density and path length distributions in Cu+Cu and Au+Au collisions I_{AA} is found to be the same within errors at the same N_{part}.

The system size dependence of I_{AA} in Figure 11 is also compared with two model calculations. The first one, the Parton Quenching Model (PQM) [52, 53], uses the Salgado-Wiedemann quenching weights [54] and a Glauber-overlap geometry where the local density scales with binary collisions. The PQM calculations are shown for three values of the transport coefficient ($\hat{q}$). The second model, the Modified Fragmentation Model (MFM), is a next-to-leading order QCD calculation with modified fragmentation functions from a higher-twist formalism [55]. The MFM uses hard-sphere geometry and the local participant density scaling [56]. We note that the MFM model has been tuned to the STAR di-hadron correlation measurements in central Au+Au collisions [5]. As can be seen, the PQM and MFM models predict rather different system size dependences of I_{AA}. While MFM predicts I_{AA} values that are independent of the collision system at a certain N_{part}, in line with the data, the PQM predictions show a clear difference between Cu+Cu and Au+Au

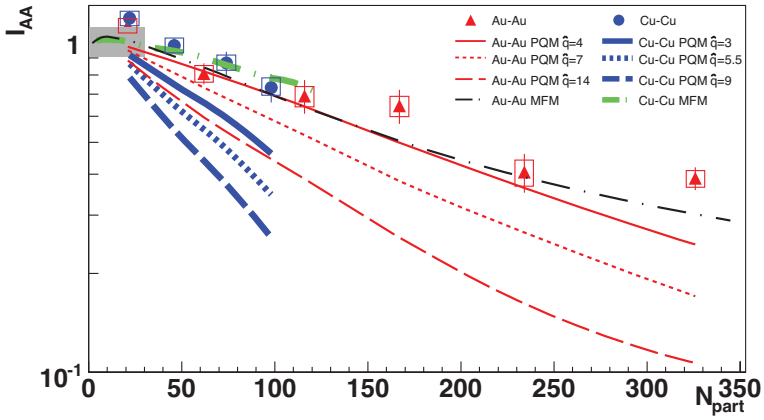

Figure 11: Centrality (N_{part}) dependence of the away-side I_{AA} for 6 GeV/c $< p_T^{trig} <$ 10 GeV/c charged trigger particles and 3 GeV/c $< p_T^{assoc} < p_T^{trig}$ associated charged particles [51]. The error bars represent statistical errors and the boxes represent the point-to-point systematic errors. The gray band represents the correlated error due to the statistical error in the d+Au data. The lines represent calculations using the PQM [52, 53] and MFM [55, 56] models. The values of $\hat{q}$ are expressed in GeV^2/fm.

collision systems for similar N_{part}. Further model studies with realistic evolution of the medium are therefore required to disentangle effects from energy loss and medium density profiles.

4. Summary and outlook

We reported recent results from the STAR experiment focussing on in-medium modifications of di-hadron correlations in A+A collisions at RHIC energy. In particular, we discussed properties of the ridge which accompanies the near-side jet-like correlation in central A+A collisions. In many aspects the ridge properties (transverse momentum spectra, particle composition) are found to be close to those of particles produced in the bulk. In addition, the sensitivity of the ridge to path length effects, the observation of a uniform distribution of associated particles in three-particle $(\Delta\eta_1, \Delta\eta_2)$ correlation studies, and the independence of jet-like/ridge yields on collision energy provide further constraints on the physical origin of the ridge. The shape modification of the away-side correlation peak was investigated using two- and three-particle correlation techniques. Using a two component analysis method evidence for a conical emission in central Au+Au collisions at $\sqrt{s_{NN}}$ =200 GeV was found. Finally, we discussed the system size dependence of high-p_T di-hadron correlations in order to get further insight into the path length dependence of partonic energy loss. Although the density and path length distributions in Cu+Cu and Au+Au collisions are different, I_{AA} was found to be the same at the same N_{part}.

We refer the reader to other presentations of STAR data related to high-p_T physics which were presented in other talks at this workshop and are therefore not covered in this paper. The results obtained from a multi-hadron ('2+1') correlation technique were discussed in [57] and in the future will enable STAR to access the medium properties in a more controlled way. Due to geometrical biases the correlation measurements have only a limited sensitivity to medium properties. Therefore, the results for direct γ-hadron correlations discussed in [58] and their future studies with even

higher statistics will provide a unique tool for investigation of partonic energy loss. The STAR experiment has also recently reported the first measurements of fully reconstructed jets in heavy-ion collisions which will allow e.g. a direct access to the medium modification of fragmentation functions. The discussion of this topic is summarized in [59].

Acknowledgments

The work has been supported by the IRP AVOZ10480505, by the Grant Agency of the Czech Republic under Contract No. 202/07/0079, and by the grants LC07048 and LA09013 of the Ministry of Education of the Czech Republic.

References

[1] S. S. Adler *et al* (PHENIX), *Phys. Rev. Lett.* **91**, 172301 (2003).

[2] J. Adams *et al* (STAR), *Phys. Rev. Lett.* **92**, 052302 (2004).

[3] B. I. Abelev *et al* (STAR), *Phys. Rev. Lett.* **97**, 152301 (2006).

[4] B. I. Abelev *et al* (STAR), *Phys. Lett.* **B655**, 104 (2007).

[5] J. Adams et al. (STAR) , *Phys. Rev. Lett.* **97**, 162301 (2006).

[6] S. Salur *et al* (STAR), arXiv:0809.1609.

[7] J. Putschke *et al* (STAR), arXiv:0809.1419.

[8] J. Putschke *et al* (STAR), *J. Phys.* **G34**, S679 (2007).

[9] C. Adler *et al.* (STAR), *Phys. Rev. Lett.* **90**, 082302 (2003.

[10] J. Adams *et al.* (STAR), *Phys. Rev. Lett.* **95**, 152301 (2005).

[11] J. Bielcikova *et al* (STAR), *J. Phys.* **G34**, S979 (2007).

[12] C. Nattrass *et al* (STAR), arXiv:0804.4683[nucl-ex].

[13] C. Nattrass *et al* (STAR), these proceedings.

[14] C. Suarez *et al* (STAR), poster presented at Quark Matter 2008 conference.

[15] C. B. Chiu, R. C. Hwa, *Phys. Rev. C* **72**, 034903 (2005).

[16] R. C. Hwa, arXiv: 0904.2159.

[17] A. Feng *et al.* (STAR), *J. Phys.* **G35**, 104082 (2008).

[18] P. K. Netrakanti *et al* (STAR), *J.Phys.* **G35**, 104010 (2008).

[19] R. C. Hwa and Z. Tan, *Phys. Rev.* **C72**, 057902 (2005).

[20] N. Armesto, C. A. Salgado, U. A. Wiedemann, *Phys. Rev. Lett.* **93**, 242301 (2004).

[21] A. Majumder, B. Mueller, S. A. Bass, *Phys. Rev. Lett.* **99**, 042301 (2007).

[22] C.-Y. Wong, *Phys.Rev.* **C76**, 054908 (2007).

[23] S.A. Voloshin, *Nucl. Phys.* **A749**, 287 (2005).

[24] E.V. Shuryak, *Phys.Rev.* **C76**, 047901 (2007).

[25] C. A. Pruneau, S. Gavin, S.A. Voloshin, *Nucl. Phys.* **A802**, 107 (2008).

[26] A. Dumitru, F. Gelis, L. McLerran, R. Venugopalan, arXiv: 0804.3858.

[27] S. Gavin, L. McLerran, G. Moschelli, arXiv:0806.4718.

[28] S. S. Adler *et al.* (PHENIX), *Phys. Rev. Lett.* **97**, 052301 (2006).

[29] H. Stoecker, *Nucl. Phys.* **A750**, 121 (2005).

[30] J. Casalderrey-Solana, E. V. Shuryak, D.Teaney, *J. Phys. Conf. Ser.* **27**, 23 (2005).

[31] I. Vitev, *Phys. Lett.* **B630**, 78 (2005).

[32] A. D. Polosa and C.A. Salgado, *Phys.Rev.* **C75**, 041901 (2007).

[33] I. M. Dremin, *Nucl. Phys.* **A767**, 233 (2006);

[34] V. Koch, A. Majumder, X.-N. Wang, *Phys. Rev. Lett.* **96**, 172303 (2006).

[35] J. Ulery and F. Wang, *Nucl. Instrum. Meth.* **A595**, 502 (2008).

[36] J. Ulery, *et al.* (STAR), *Nucl. Phys.* **A774**, 581 (2006).

[37] J. Ulery *et al.* (STAR), *Nucl.Phys.* **A783**, 511 (2007).

[38] J. Ulery *et al.* (STAR), *Int.J.Mod.Phys.* **E16**, 2005 (2007).

[39] B. I. Abelev *et al* (STAR), *Phys. Rev. Lett.* **102** 052302 (2009).

[40] N. N. Ajitanand *et al.*,*Phys.Rev.* **C72**, 011902 (2005).

[41] N. Borghini, *Phys. Rev.* **C75**, 021904 (2007); N. Borghini, *J. Phys. Conf. Ser.* **110**, 032005 (2008).

[42] C. Pruneau, *Phys. Rev.* **C74**, 064910 (2006).

[43] C. Pruneau *et al.* (STAR), *J.Phys.* **G34**, S667 (2007).

[44] C. Pruneau *et al.* (STAR), *Int.J.Mod.Phys.* **E16**, 1964 (2007).

[45] R. Baier, Y.L. Dokshitzer, S. Peigne, D. Schiff, *Phys. Lett.* **B345**, 277 (1995).

[46] R. Baier, Y.L. Dokshitzer, A. H. Mueller, S. Peigne, D. Schiff, *Nucl. Phys.* **B483**, 291 (1997).

[47] R. Baier, Y.L. Dokshitzer, A. H. Mueller, S. Peigne, D. Schiff, *Nucl. Phys.* **B484**, 265 (1997).

[48] T. Renk, *Phys. Rev.* **C76**, 064905 (2007).

[49] T. Renk, K. Eskola, *Phys. Rev.* **C75**, 054910 (2007).

[50] H. Zhang, J. F. Owens, E. Wang, X.-N. Wang, *Phys. Rev. Lett.* **98**, 212301 (2007).

[51] B. I. Abelev, *et al* (STAR), arXiv:0904.1722.

[52] C. Loizides, *Eur. Phys. J.* **C49**, 339 (2007).

[53] A. Dainese, C. Loizides, G. Paic, *Eur. Phys. J.* **C38**, 461 (2005).

[54] C. A. Salgado, U. A. Wiedemann, *Phys. Rev.* **D68**, 014008 (2003).

[55] X. N. Wang, *Phys. Lett.* **B595**, 165 (2004).

[56] X. N. Wang, *Phys. Rev. Lett.* **98**, 212301 (2007).

[57] O. Barannikova, these proceedings.

[58] A. Hamed *et al* (STAR), these proceedings.

[59] J. Putschke, these proceedings.